XAS Techniques to Determine Catalytically Active Sites in Zeolites: The Case of Cu-Zeolites

XAS techniques to determine catalytically active sites in zeolites: the case of Cu-zeolites

Jeroen A. van Bokhoven,[1,2] Carlo Lamberti[3,4]

[1] Institute for Chemical and Bioengineering, ETH Zürich, CH-8093 Zurich, Switzerland
[2] Swiss Light Source, Paul Scherrer Institute, CH-5232 Villigen PSI, Switzerland. E-mail: j.a.vanbokhoven@chem.ethz.ch / jeroen.vanbokhoven@psi.ch
[3] Southern Federal University, Zorge Street 5, 344090 Rostov-on-Don, Russia.
[4] Department of Chemistry, CrisDi Centre for crystallography, University of Torino, Via Giuria 7, I-10125 Torino, Italy. E-mail: carlo.lamberti@unito.it

1. Introduction

Oxide materials find widespread application in industry, for example as semi-conductor, solar cell, catalyst, and sensor. New materials and applications continue being reported, which is a main driver for technological development and slowly making our society more sustainable. The function of these materials strongly depends on their structure, which is why their structural characterization receives much attention.

Zeolites are an important class of microporous crystalline oxides and they find widespread application as catalyst and catalyst support.[1-3] Within the refinery, they are the dominant catalysts, because of their unique structure, guaranteeing shape-selectivity, and thermal stability. Zeolites are crystalline alumina-silicates. They are micro-porous and therefore have very large surface areas. Silicon and aluminum atoms are tetrahedrally coordinated by bridging oxygen atoms.[4,5] Because there is a charge imbalance for every framework aluminum, cations are located in the zeolite pores, for each aluminum one cationic charge.[6] These cations give zeolites their catalytic function, such as a Brønsted acid in case of proton-exchanged zeolites and Lewis or redox function in case of cations,[7] such as iron[8] and copper. These extra-framework species catalyze a wide range of redox reactions, notably oxidation. Unique features are their stability, induced by the space-restricting functionality of the pores and their ability to perform oxidation reactions selectively.[9-14] Instead of aluminum, other atoms may replace silicon, which imply different activity: redox chemistry is for example done over titanium containing Ti-silicalite.[15-17] Figure 1 illustrates a zeolite structure, notably zeolite Y or faujasite with its preferred extra-framework cation sites.

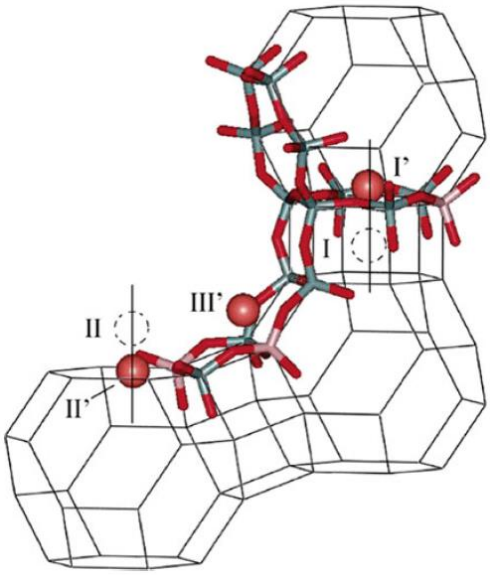

Figure 1. Schematic picture of zeolite Y. Gray and pink identify the location of silicon respectively aluminum atoms, which are connected by bridging atoms, forming the crystalline framework. The red and dashed spheres illustrate possible and preferred locations for extra-framework ions. The faujasite structure is composed of sodalite cages, of which three are shown here. They are connected by double six-rings. The maximal pore size in faujasite contains twelve T-atoms and has a size of 7.4 Å. The largest accessible cage has a diameter of 12 Å. Adapted with permission from Ref. [18], copyright American Chemical Society (2006).

X-ray absorption-based methods have played an important role in determining the structure of the framework and extra-framework species in the zeolite structure, as recently summarized.[17] X-ray-based techniques are attractive, because of their versatile applicability.[19-23] They yield electronic and geometric structures and can be applied under in situ conditions. Thus, a functioning material, such as a sensor, battery,[24] catalyst,[25] etc. can be structurally characterized while it performs its function. This chapter concerns the structure of extra-framework copper species in zeolites as determined by X-ray based spectroscopic methods. The focus is on copper-based zeolites, because of their large academic and commercial interest.

Copper-exchanged zeolites enjoy large academic and industrial interest. They are active catalysts for selective catalytic reduction (SCR), which converts nitrogen oxides into di-nitrogen and water.[26-31] This reaction finds widespread application in stationary and mobile exhaust control. Diesel engines on ships, trains and automobiles contain SCR catalysts, which consist of base metal oxides, such as tungsten, vanadium, and molybdenum, of precious metals, or of transition metal ions on zeolite supports. One of the most-studied ones is copper-exchanged zeolites.[32] Contemporary research focuses on the reaction mechanism and the identification of the catalytically active sites that are responsible.[28-31] Here, in situ and operando x-ray absorption measurements are reviewed to provide the state of the art in site and mechanism elucidation.

A second major research field of copper-exchanged zeolites is the selective conversion of methane to methanol. Because of the higher reactivity of methanol compared to methane, the direct conversion of methane to methanol using oxygen is restricted to low conversion, because of carbon dioxide formation.[33] For this reason, methane is commercially converted into methanol via syngas production and its subsequent conversion into methanol.[34,35] Such process is cost intensive and not suitable for small-scale operation. Methane is abundantly available, however, often at stranded locations and therefore flared, observable from outer space by pictures of the earth by night. An equivalent to one quarter of the European energy use is put to waste. Direct conversion of methane into a liquid, such as methanol, would enable transporting it, and making its conversion into fuels or chemicals possible, representing an enormous increase in value.

2. Brief historical overview

Copper-exchanged zeolites have been widely investigated after the discovery in the early nineties by the Iwamoto group[32,36,37] and by Li and Hall[38,39] that Cu-ZSM-5 are active in the direct decomposition of nitric oxide to nitrogen and oxygen.[40] The study of this catalytic process has deserved a great practical interest, as nitric oxides are known to be a major cause of air pollution.[41] Successively, other Cu-exchanged zeolites have shown to be active in the selective catalytic reduction of NOx such as: MOR, X, Y, USY, IM5 etc. X-ray absorption spectroscopies, both XANES and EXAFS played a key role in the investigation of the coordination and oxidation state of copper species in such systems in the activated forms and under different reaction conditions.[42-50]

More recently, the Cu-exchanged form of the novel SSZ-13 zeolite, with CHA framework and high Si/Al ratio, is attracting a lot of attention due to its outstanding performance in NH_3-assisted selective catalytic reduction (SCR) of NO_x gases contained in the exhaust fumes from cars and industrial plants, in terms of activity and hydrothermal stability.[26,27] In order to explain such behavior and to develop the NH_3-based SCR reaction mechanism many studies were performed by the groups all over the world involving a very broad range of characterization techniques, such as FTIR,[7,51] UV-

Vis,[51] EPR,[51] XRD[52] and so on, as recently reviewed by Beale et al.[53] Among them X-ray spectroscopy (both absorption[19,54] and emission[55]) is particularly useful due to its element selectivity, since the active sites of SCR reaction in Cu-SSZ-13 are low-abundance Cu ions hosted without any long-range order in the cavities of the zeolite framework. Careful analysis of EXAFS, XANES and XES spectra, often assisted by the advanced DFT calculations, yields detailed information on the local environment and oxidation state of Cu centers in different reaction conditions.[30,31,53,56-60] *In situ* and *operando* studies, possible due to the high penetration depth of the hard X-rays (around 9 keV, corresponding to the Cu K-edge), provide the means to answer "chemical questions" concerning the reactivity of the Cu species towards particular gases at given temperatures, which is crucial for determining different steps of the reaction mechanism.[19-21,54]

The structure of the Cu-CHA framework has been known since the seventies from the single crystal diffraction studies,[61] that of Cu-SSZ-13 is similar, just with a lower Al and Cu content. It is composed of double six-membered rings (6-rings) connected in an AABBCC sequence, forming cavities with eight-membered windows (8-rings), see Figure 2.

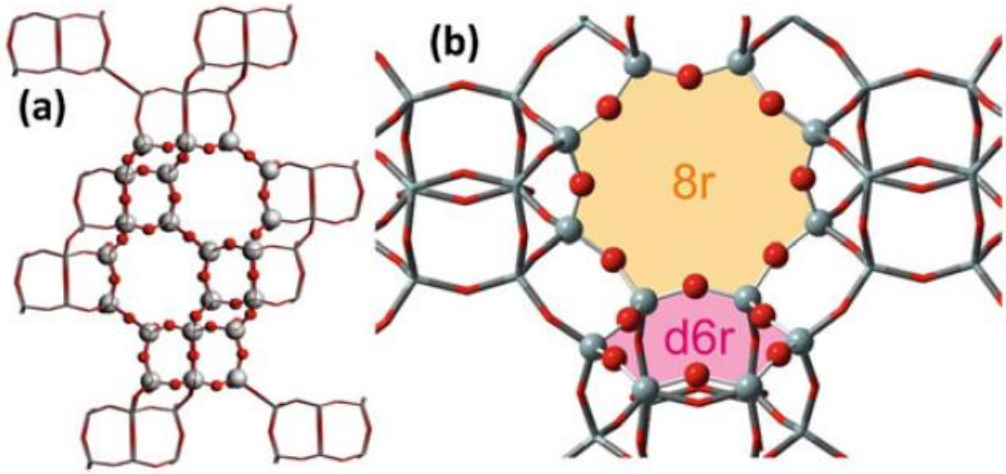

Figure 2. Part (a): sticks representation of a fragment of CHA framework with the atoms forming the large cavity highlighted with balls. Part (b): zoom of the large CHA cavity showing 6- and 8-membered rings, which are reported to be the most likely hosts for Cu ions. Color code: Si – gray, O – red.

3. Determination of the local environment of Cu in SSZ-13 upon activation

Once Cu-SSZ-13 has shown its outstanding catalytic properties,[26,27] the focus of the structural investigations was gradually shifted from the framework to the location of the isolated Cu ions in the hydrated and thermally activated material, which are the active sites of the SCR reaction. One of the first studies, carried out by Fickel and Lobo demonstrated that the Cu ions tend to occupy the centers of the 6-rings.[52] Since every 6-ring is likely to have one negatively charged tetrahedral unit with Al substituting Si, the authors admitted, that Cu cations are expected to be shifted towards it from the center of the ring. However, XRD refinement was always converging to central position due to the lack of structural contrast. Nonetheless, it was possible to detect that, being always "projected" on the center of the 6-ring, the Cu ions were gradually approaching its plane upon calcination. The authors suggested that this effect may take place due to the dehydration of the Cu ions.

Successively, Korhonen *et al.* presented Cu K-edge EXAFS data for both calcined and as-synthesized (hydrated) Cu-CHA[62] and analyzed the data using as starting model the previous theoretical structure of Cu in the 6-ring reported by Pierloot et al.[63] The fit resulted in adequate agreement with the experiment, confirming that Cu is indeed situated off-axis of the 6-ring. The very substantial shift of one of the oxygens in the 6-ring from the initial position during fitting was explained by the lower degree of deformation of the ring compared to the one predicted by DFT. First shell coordination numbers were determined as 4 for hydrated material and 3.2 for the calcined one.

Presented XANES results also indicated the decrease of coordination upon dehydration due to the decrease of the main maximum (the white line). Later the shift of the Cu ion from the center of the 6-ring was also confirmed by Deka *et al.*,[64] by means of XANES simulations. Calculated spectrum of the model with Cu placed off-axis resulted in a much better agreement with the experimental data compared to the centered model.

Hydration issue was raised in more detail in the work of McEwen *et al.*[56] where it was demonstrated that Cu K-edge XANES spectrum of the as-synthesized Cu-SSZ-13 zeolite is very similar to the one of aqueous solution of Cu ions. This was further confirmed by Borfecchia *et al.*,[60] who presented also a comparison of the EXAFS data for these two cases. High degree of similarity of both XANES and EXAFS data suggests that as long as the zeolite is exposed to air at room temperature, copper is covered by a shell of water molecules. Such shielding explains the lack of the framework contribution to the EXAFS data of the hydrated material and confirms the initial hypothesis of Fickel and Lobo.[52] At the same time, a substitution of one H_2O molecule by OH^- group cannot be excluded since these species are hardly distinguishable in EXAFS.

One of the most extensive spectroscopic studies of the Cu-SSZ-13 (Cu/Al=0.444, Si/Al=13.1) activation to date was carried out by Borfecchia *et al.*,[60] who followed the activation in temperature up to 400 °C in both O_2/He and pure He flows with XANES, EXAFS and valence-to core XES spectroscopies. EXAFS-optimized experimental setup and rather high copper content in the sample allowed to achieve a very good data quality paving the way to a detailed quantitative analysis. XANES, EXAFS and valence to core XES spectra, together with the optimized DFT models and corresponding XANES and XES simulations are reported in Figure 3 and Figure 4 for O_2- and He-activated samples, respectively. Borfecchia *et al.*,[60] tried several DFT models sitting Cu(II), or Cu(I), in the 8r or in the 6dr rings and inserting either one or two Al atoms in the T positions of the ring. Structures reported in Figure 3c and Figure 4c,d are only those that are compatible with the experimental results.

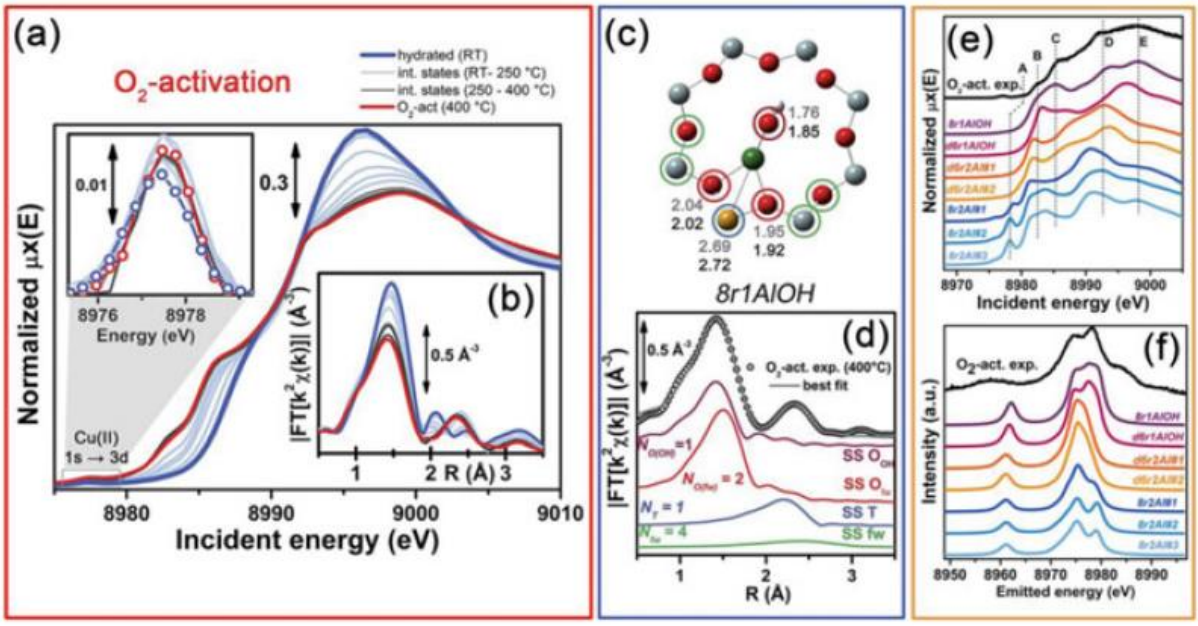

Figure 3. Part (a): *XANES spectra following the activation from room temperature (blue curve, hydrated material) to 400 °C (red curve, activated material) of Cu-SSZ-13 in 50% O_2/He flow. The inset shows a magnification of the 1s→3d transition, typical of Cu(II) species. Part (b) as part (a) for the k^2-weighted FT of the EXAFS spectra. Part (c): DFT model of the dominant Cu-site in the O_2-activated material. Part (d): best EXAFS fit and related main individual components obtained using the model reported in part (c). Part (e): experimental HERFD XANES spectrum (black curve) and computed XANES spectra (colored curves) for the different optimized possible sites. Part (f): as pat (e) for the valence*

to core XES spectra. Both HERFD XANES and XES simulations support the EXAFS results. Adapted with permission from Borfecchia *et al.* [60], copyright Royal Society of Chemistry (2015).

Upon activation in O_2/He flux Cu(II) centers undergo progressive dehydration, while interacting more closely with the framework, keeping +2 oxidation state. Features typical for Cu(II) in low-symmetry environment were observed in XANES (Figure 3a), while EXAFS witnesses the marked decrease of the first shell intensity due to the loss of the coordinated water molecules (Figure 3b). Comparable evolution of the XANES spectra upon similar activation in oxidative environment was observed also by Kwak *et al.*[65] Conversely, as already observed for Cu(II)-ZSM-5[48] and for Cu(II)-MOR[66] systems, upon activation in vacuum or in inert atmosphere (e.g. He flux) the Cu oxidation state did change to +1, as evidenced for the Cu(II)-SSZ-13 system by the disappearance of 1s→3d transition and by the additional redshift of the edge, see Figure 4a. Most interestingly, the high-quality EXAFS data reveal that the coordination of Cu upon He-activation was further decreased compared to the activation in O_2. Coupled with the observation that the reduction in He flow appears only at high temperature (T > 250 °C), while at lower T the evolution of the spectra is identical to the O_2-activation case, it indicates that a charged extra-ligand is still coordinated to Cu even at high temperature in case of O_2-activation. This evidence support the hypothesis of the presence of an OH^- ligand in the first coordination shell of Cu(II) as advanced in the IR study of Giordanino *et al.*[51] to assign the ν(OH) stretching mode at 3657 cm^{-1}.

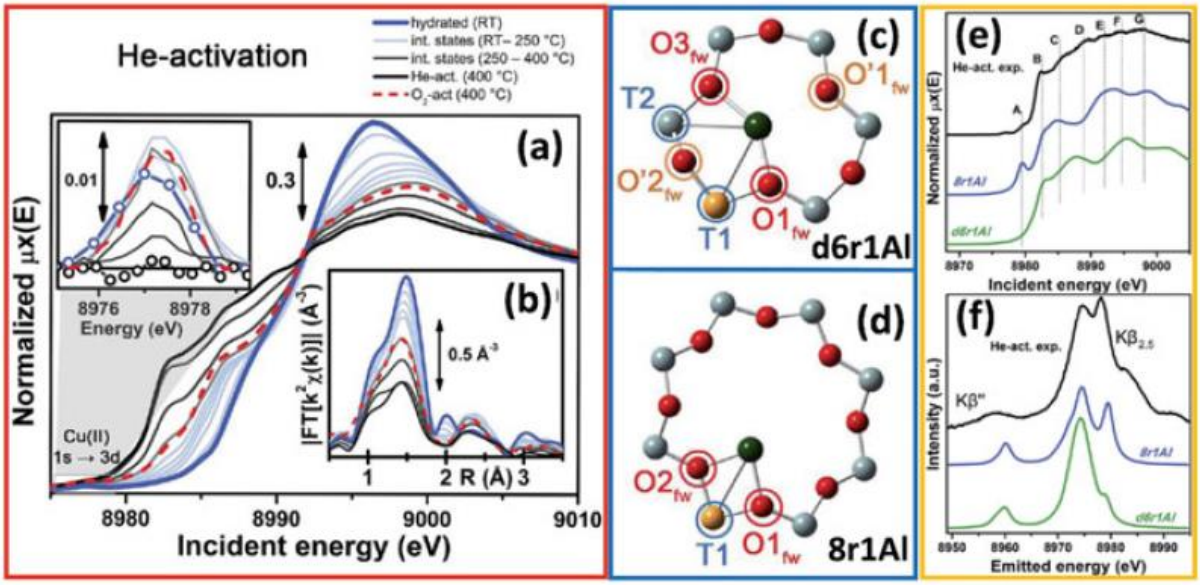

Figure 4. Part (a): *XANES spectra following the activation from room temperature (blue curve, hydrated material) to 400 °C (red curve, activated material) of Cu-SSZ-13 in inert He flow. The inset shows a magnification of the 1s→3d transition, typical of Cu(II) species and disappearing at high temperature. Part (b) as part (a) for the k^2-weighted FT of the EXAFS spectra. Parts (c,d): DFT model of the dominant Cu-sites in the He-activated material. Best EXAFS fit and related main individual components obtained using the model reported in part (c). Part (d): experimental HERFD XANES spectrum (black curve) and computed XANES spectra (colored curves) for the different optimized possible sites. Part (f): as pat (e) for the valence to core XES spectra. Both HERFD XANES and XES simulations support the EXAFS results.* Adapted with permission from Borfecchia *et al.* [60], copyright Royal Society of Chemistry (2015).

The authors have further tested this hypothesis by performing a set of DFT simulations of Cu ions in different places of the framework and using the resulting structures as input for EXAFS fits and for the simulations of the high resolution fluorescence detected (HRFD) XANES and XES spectra, see parts (e) and (f) of Figure 3 and Figure 4. For the O_2-activated material, the best overall agreement with the experimental data was obtained for the models of Cu(II) in the 8-ring, in form of a Cu(OH) complex, see Figure 3c confirming the first assignment of the ν(OH) stretching mode at 3657 cm^{-1}.[51].

While in case of He-activation it was a bare Cu(I) cation hosted mainly in the 8r, with a minority occupancy of the d6r site.

4. Understanding the SCR mechanism

A large number of studies were devoted in the understanding of the SCR reaction mechanism over Cu-SSZ-13 system. In this regard remarkable efforts were invested into measuring XAS and XES spectra in different reaction-relevant conditions. We can divide such studies into two families The first concerns experiments in truly *operando* conditions, when the sample is exposed to the complete reaction mixture (including NO, NH_3, O_2, He, H_2O, in some studies also NO_2 and CO_2) under controlled temperature. Most often such studies are performed in plug-flow reactors, such as the one described in the work of Kispersky *et al.*,[67] collecting XAS and XES spectra of the catalyst in different reaction-relevant conditions. The interpretation of such data is intrinsically complicated, since several different Cu species forming on the different stages of the reaction may simultaneously contribute to the signal. The common approach to analyze such data is to measure also the spectra of the relevant reference materials, and, performing linear combination analysis, determine the relative contribution of each species to the spectrum of the catalyst under SCR conditions. Such strategy was adapted in the works of McEwen *et al.*[56] and of Bates *et al.*,[57] where the samples with different Cu loadings were tested. Fitting the data with the Cu(I) and Cu(II) standards allowed the authors to determine the ratio between the amounts of Cu species of these oxidation states during the reaction.

The second strategy consists in probing separately different stages of SCR reaction thus testing the independently developed hypotheses regarding the behavior of the active sites in particular conditions. Such approach allowed Janssens et al.[31] to decouple the oxidation and reduction stages of the suggested SCR cycle, see Figure 5. In particular, the authors have tested the effect of different red-ox agents, namely NO + O_2 mixture (gray cirve), O (orange curve), NH_3 (blue curve) and their mixture (red curve), see Figure 5a,b. The results clearly indicate that almost complete reduction occurs only after exposure to the mixture of NO and NH_3. Resulting spectrum is characteristic for $Cu^+(NH_3)$ species in linear geometry.[51] Conversely, NO alone is not able to reduce Cu^{2+}. Exposure to NH_3 leads only to a partial reduction accompanied by the formation of a linear Cu complex, while around 75% of Cu species remain oxidized, presumably forming a planar tetra-ammino complexes.[31]. This study also revealed that the interaction of Cu(I) species with NO_2 and NO+O_2 results in the same Cu(II) species, see Figure 5c, in agreement with the suggested mechanism, see Figure 5d.

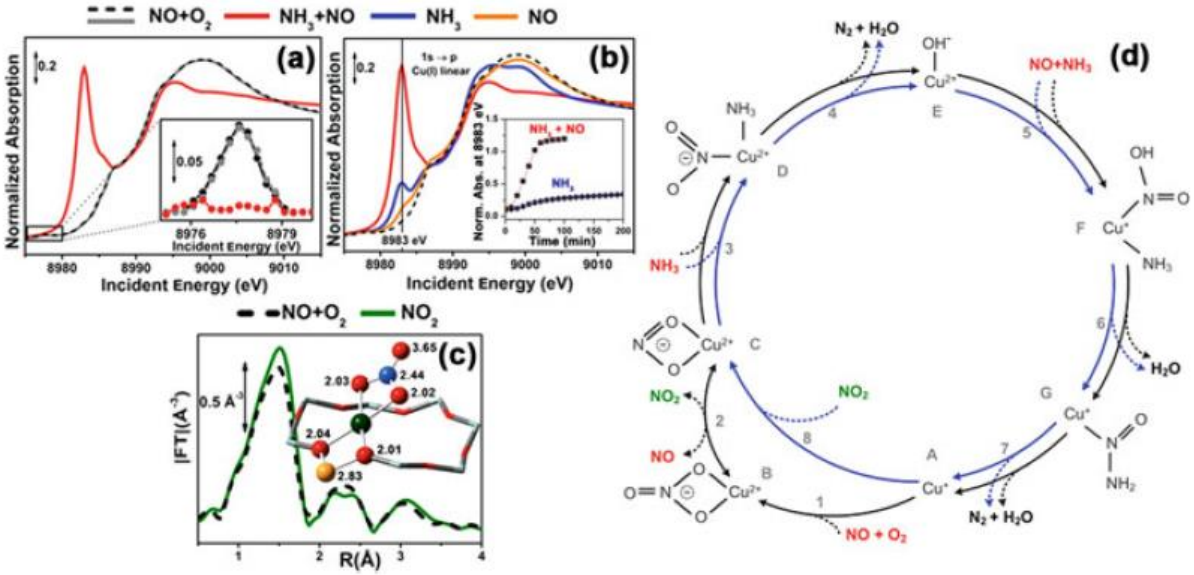

Figure 5. In situ Cu K-edge XAS data collected at 200 °C under different SCR-relevant conditions. Part (a): XANES spectra upon initial oxidation in 1000 ppm NO + 10% O_2 (dashed black curve), reduction in 1200 ppm NH_3 + 1000 ppm NO (solid red curve) and re-oxidation in 1000 ppm NO + 10% O_2 (solid grey curve). Part (b): XANES spectra showing

the reducing capability of 1200 ppm NH_3 (solid blue curve), 1000 ppm NO (solid orange curve) and a mixture of 1200 ppm NH_3 with 1000 ppm NO (solid red curve) on the Cu(II) state obtained after initial oxidation in a mixture of 1000 ppm NO and 10% O_2 (dashed black curve). Part (c): Fourier-transformed EXAFS after exposure of dehydrated Cu-SSZ-13 to 1000 ppm NO_2 (solid green curves), and to a mixture of 1000 ppm NO and 10% O_2 (dashed black curve) together with the structural model of the bidentate Cu-NO_3^- species forming at these conditions. Part (c): catalytic SCR cycle. The fast SCR cycle is represented in the blue internal loop, and the NO activation cycle is represented in black. Reactants are indicated in red, reaction products are indicated in black, and the NO_2 intermediate is indicated in green. Adapted with permission from Ref. [31], Copyright American Chemical Society (2015).

The obtained complex was a bidentate Cu-NO_3^-, as evidenced by the EXAFS and XANES analysis. There here-reported XAS and XES data, supported by parallel IR, EPR and DFT studies confirm the proposed scheme of the SCR reaction, resulting in greatly improved understanding of its chemistry.

A similar strategy of probing particular intermediate states of the reaction was adapted by the group of Grunwaldt[30] who used valence to core XES and HERFD XANES for characterizing different stages of SCR reaction. It was possible to detect the formation of Cu-N bond upon coordination of NH_3 monitoring the shift of Kβ" satellite from 8956.9 to 8958.3 eV. Notably, no such shift was observed in the cases when NH_3 was absent from the feed, indicating thus the very weak coordination of NO to Cu accompanied by minor changes in Cu local environment.[30]

Summarizing, in the past five years, due to the efforts of several independent research groups, there has been a marked advance in the understanding of the structure and reactivity of the active sites in Cu-SSZ-13 catalyst. As shown in this section, significant part of the insights were gained by the element-selective XAS/XES studies, complemented by laboratory techniques and supported by DFT calculations. Several mechanisms of SCR reaction catalyzed by Cu-SSZ-13 were proposed based on the results of such multi-technique investigations.[28-31] Although there are still some contradictions in the literature regarding the stages of the reaction and the formed intermediates, there is no doubt that these issues will be eventually resolved in the coming up studies.

5. Methane to methanol over copper exchanged zeolites

As mentioned, the direct conversion of methane to methanol is very attractive, however difficult. Over the years, a stepwise, chemical looping reaction has been developed over copper-exchanged zeolites.[68-70] The fundamental principle is to stabilize any intermediate from methane, which is thus prevented from further reacting.[32] The first such system is that of Periana,[71] which is based on platinum bidiazine, which reacts methane to form a methyl ester. In a subsequent step, the methanol is produced. Analogously, in the Cu-zeolite, after high temperature activation in oxygen, methane is reacted between 425 to 475 K and the thus formed intermediate remains adsorbed on the catalyst surface. Methanol can be extracted by liquid phase extraction[13] or desorbed by steam. Nature is able to selectively convert methane into methanol based on iron respectively copper systems.[72,73] Such systems have served as inspiration for active sites in the zeolites.[74]

Table 1. Copper coordination over-exchanged Cu-ZSM5 (Si/Al = 12) from EXAFS fitting. Adapted with permission from Ref. [75], copyright American chemical Society (2003).

	N	R (Å)	$\Delta_{DWF}{}^1$ (Å^2)
After ion exchange			
Cu – O	4.0	1.96	-0.001
Cu --- Al	0.7	3.18	0.008
Treated in inert at 773 K			
Cu – O	2.3	1.92	0.006
Cu --- Cu	0.5	2.84	0.015
After calcination 623 K			
Cu – O	4.1	1.95	0.002
Cu --- Cu	0.9	2.87	0.009
Cu --- Al	0.8	3.21	0.006

[1] Debye-Waller factor, relative to the reference

Following the work on reduction of copper in Cu-ZSM-5 by Yamaguchi et al.[76-78] Groothaert et al.[75] measured the structure of copper in ZSM-5 (over-exchanged, Si/Al = 12) during treatment in inert respectively oxygen. After ion exchange, copper(II) ions were four-coordinated with oxygen atoms without evidence of copper – copper coordination (Table 1). Instead, a contribution of aluminum of the framework was found. Heat treatment in helium at 773 K caused the oxygen coordination number to about half its original and a copper – copper coordination of 0.5 was observed. The Cu K edge XANES showed the characteristic pre-edge of copper(I), which is indicative of copper auto-reduction. Heating in the presence of oxygen instead of inert maintained the copper oxidation state of two and the EXAFS fitting identified an oxygen coordination of four, a copper – copper coordination of one and copper – aluminum of one. Distinction between the latter two was done on the basis of combined k^0 and k^3 weighting of the fits. In the absence of a copper – copper coordination, the Debye-Waller factor of the copper – aluminum contribution decreased to unrealistic negative values, which is indicative of 'making it look like a copper scatterer'.

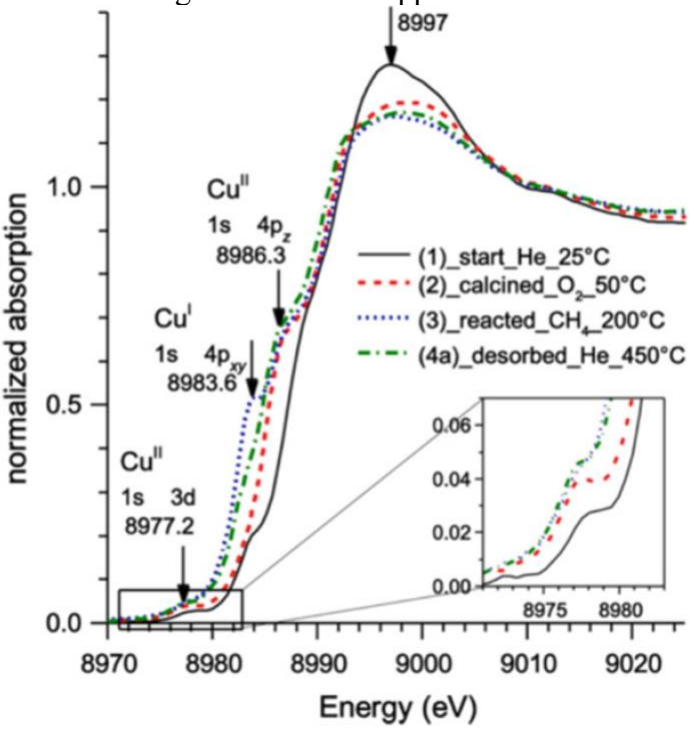

Figure 6. Cu K edge XANES of Cu-MOR (1) directly after ion exchange, (2) after high temperature calcination, (3) after reaction with methane, and (4) after high temperature desorption in inert. The temperature of measurement is given next to the sample name. The insert highlights the pre-edge region. Heating in inert causes autoreduction of copper(II); calcination yields copper(II), and subsequent reaction with methane reduction of a large fraction into copper(I). Reproduced with permission from Ref.[69], copyright American Chemical Society (2014).

The copper – copper coordination is indicative of formation of copper dimers or of a mixture of monomers and oligomers. Based on complementary UV-vis data, a bis(μ-oxo) dicopper core was proposed. Earlier and later proposals have suggested the formation of a mono μ-oxo core to be more likely.[74,79] Based on theory and essentially similar EXAFS data, instead of the copper dimer, a trimer has been suggested very recently.[80] Whatever the exact nature of the oxygen-activated species, they react with methane, which, after extraction in liquid[11] or by steam[68] yields methanol.

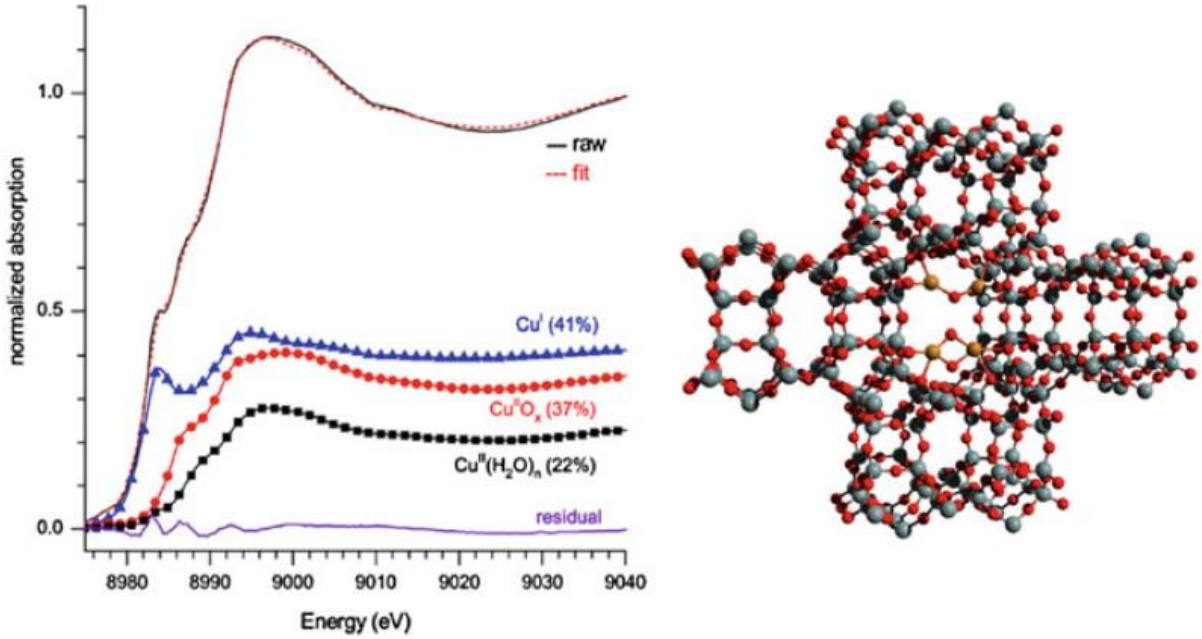

Figure 7. (left) Measured spectrum and deconvoluted Cu K edge spectra of Cu-MOR after high temperature oxygen activation and subsequent reaction with methane. Reproduced with permission from Ref.[69], copyright American Chemical Society (2014). (right) Depiction of the 12-membered ring in mordenite with a mono μ-oxo dicopper respectively bis μ-oxo dicopper core; the copper atoms are given in gold.

The reaction of the oxygen-activated copper catalyst with methane has been studied by in situ quick x-ray absorption spectroscopy. Figure 7 shows the Cu K edge XANES spectra of copper-exchange mordenite after ion exchange (1), calcination in oxygen (2), reaction with methane (3), and helium treatment at elevated temperature. The initial copper structure is conform literature and assigned to hydrated copper(II) ions. Calcination leads to oxygenated and active copper(II) sites, indicative of the bis- respectively mono-μoxo dicopper core. Reaction of these species with methane yielded a distinct pre-edge feature at 8983.6 eV, attributed to the 1s $\rightarrow$ 4p transition of copper(I). Quantification by linear combination fitting yielded a mixture of copper(I) : copper(II) oxide : hydrated copper(II) of 41 : 37 : 22 (Figure 7). Stable (Cu^{I}-OCH_3-Cu^{II}) and (Cu^{I}-OH-Cu^{II}) were identified as possible stable intermediates by DFT.[74]

During admission of steam to the methane activated sample, methanol was detected in the mass spectrometer and the concomitant formation of hydrated copper(II), some copper(II) oxide and the loss of the copper(I) (Figure 8). The changes in the electronic structure were paralleled by relatively minor changes in EXAFS, which identifies the absence of large structural changes and sintering. This enables performing a second cycle. The EXAFS analysis proved to be very complex and up to date no definite conclusions have been drawn from them.

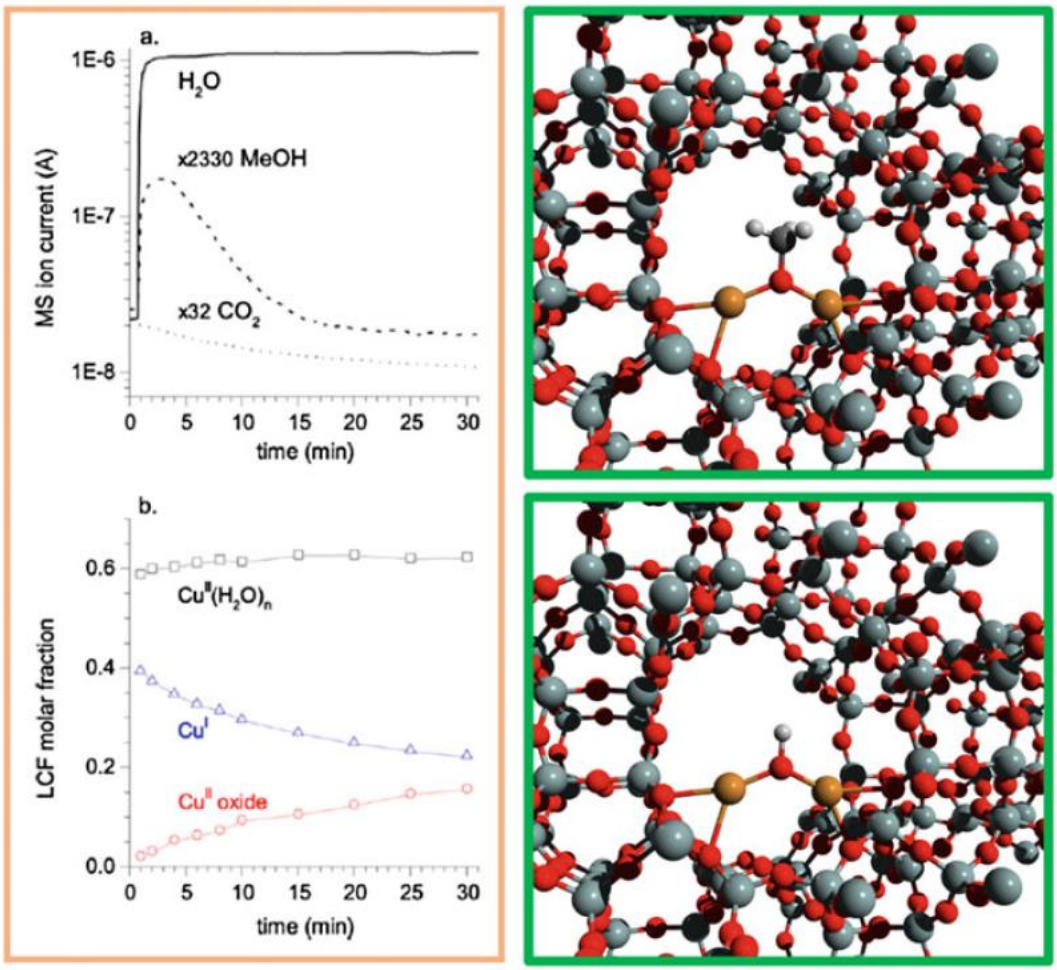

Figure 8. (left panel) a. Methanol formation identified by mass spectrometry by providing wet helium over a methane reacted Cu-mordenite catalyst after high temperature oxygen activation and (left panel) b. linear combination fitting results of the copper species upon interaction of wet helium with a methane-reacted Cu-MOR. The two measurements were performed simultaneously. Reproduced with permission from Ref.[69], copyright American Chemical Society (2014) (right panel) A possible dicopper core with a bridging methoxy (top) and hydroxyl group, calculated to be possible stable intermediates.

Overall, oxygen activation of ion-exchange copper zeolites yields small copper clusters, mostly suggested to be dimers, that contain oxygen that is reactive towards methane. The thus formed intermediate is associated to the presence of coper(I) and it can be desorbed as methanol using steam. Such step-wise process is a promising route towards direct methanol production from methane,[81] even though it is currently hampered by low methanol per pass yields.

5. Conclusion

Cu-zeolites find commercial application in SCR and are promising catalysts for the direct methane to methanol conversion. X-ray absorption and emission-based techniques have played and continue to play an invaluable role in determining the structure of the catalytically active sites. In particular, the in situ and operando capacity in combination with element selectivity are decisive factors in their success. In both reactions, copper undergoes a change in redox state when cycling through the reaction; in SCR NO and NH_3 and in the direct methane to methanol it is the methane that reduces copper(II) into copper(I). Despite this similarity in redox activity, the catalytically active sites have pronounced different structures, in the former reaction, single copper ions are responsible for activity, which are inactive for methane oxidation. In that case, small clusters, mostly assumed to be oxygen bridged copper dimers and, more recently, a copper trimer, are the active species. Even though discussions about details continue, the catalytic cycle in the SCR reaction has been almost completely

established. In contrast, the intermediate that is formed upon methane interaction with the oxygen activated remains unknown and major discussions about the exact active phase continue. X-ray-based methods will continue to play a major role in further identification of active sites and catalytic cycles. Complementary experimental and theoretical characterization tools will be needed.

Acknowledgements
C.L. acknowledges the Mega-grant of the Russian Federation Government to support scientific research at the Southern Federal University, no. 14.Y26.31.0001.

References

1. Weitkamp J, Puppe L, *Catalysis and Zeolites Fundamentals and Applications*, Springer, Berlin, 1999.
2. Davis ME (2002) Ordered porous materials for emerging applications. Nature, 417: 813-821.
3. Cejka J, Corma A, Zones S, *Zeolites and Catalysis*, Wiley VCH, Weinheim, 2010.
4. Szostak RM, *Molecular Sieves*, Van Nostrand Reinhold, New York, 1989.
5. Meier WM, Olson DH, Baerlocher C, *Atlas of Zeolite Structure Types*, Elsevier, London, 1996.
6. Frising T, Leflaive P (2008) Extraframework cation distributions in X and Y faujasite zeolites: A review. Microporous Mesoporous Mater., 114: 27-63.
7. Bordiga S, Lamberti C, Bonino F et al (2015) Probing zeolites by vibrational spectroscopies. Chem. Soc. Rev., 44: 7262-7341.
8. Zecchina A, Rivallan M, Berlier G et al (2007) Structure and nuclearity of active sites in Fe-zeolites: comparison with iron sites in enzymes and homogeneous catalysts. Phys. Chem. Chem. Phys., 9: 3483-3499.
9. Panov GI, Sobolev VI, Kharitonov AS (1990) The role of iron in N_2O decomposition on ZSM-5 zeolite and reactivity of the surface oxygen formed. 61: 85-97.
10. Iwamoto M, Hamada H (1991) Removal of nitrogen monoxide from exhaust gases through novel catalytic processes. Catal. Today, 10: 57-71.
11. Smits RHH, Iwasawa Y (1995) Reaction-mechanisms for the reduction of nitric-oxide by hydrocarbons on Cu-ZSM-5 and related catalysts. Appl. Catal. B-Environ., 6: L201-L207.
12. Panov GI, Uriarte AK, Rodkin MA et al (1998) Generation of active oxygen species on solid surfaces. Opportunity for novel oxidation technologies over zeolites. Catal. Today, 41: 365-385.
13. Groothaert MH, Smeets PJ, Sels BF et al (2005) Selective oxidation of methane by the bis(μ-oxo)dicopper core stabilized on ZSM-5 and mordenite zeolites. J. Am. Chem. Soc., 127: 1394-1395.
14. Hammond C, Dimitratos N, Lopez-Sanchez JA et al (2013) Aqueous-Phase Methane Oxidation over Fe-MFI Zeolites; Promotion through Isomorphous Framework Substitution. ACS Catal., 3: 1835-1844.
15. Bordiga S, Coluccia S, Lamberti C et al (1994) XAFS study of Ti-silicalite: structure of framework Ti(IV) in presence and absence of reactive molecules (H_2O, NH_3) and comparison with Ultraviolet-Visible and IR results. J. Phys. Chem., 98: 4125-4132.
16. Bordiga S, Damin A, Bonino F et al (2007) Reactivity of TS-1 towards H2O2/H2O solutions. Prepr. Pap.-Am. Chem. Soc., Div. Pet. Chem., 52: 196-200.
17. van Bokhoven JA, Lamberti C (2014) Structure of aluminum, iron, and other heteroatoms in zeolites by X-ray absorption spectroscopy. Coord. Chem. Rev., 277: 275-290.
18. Drake IJ, Zhang Y, Briggs D et al (2006) The Local Environment of Cu^+ in Cu−Y Zeolite and Its Relationship to the Synthesis of Dimethyl Carbonate. J. Phys. Chem. B, 110: 11654-11664.
19. Bordiga S, Groppo E, Agostini G et al (2013) Reactivity of Surface Species in Heterogeneous Catalysts Probed by In Situ X-ray Absorption Techniques. Chem. Rev., 113: 1736-1850.
20. Mino L, Agostini G, Borfecchia E et al (2013) Low-dimensional systems investigated by x-ray absorption spectroscopy: a selection of 2D, 1D and 0D cases. J. Phys. D-Appl. Phys., 46: 72.
21. Garino C, Borfecchia E, Gobetto R et al (2014) Determination of the electronic and structural configuration of coordination compounds by synchrotron-radiation techniques. Coord. Chem. Rev., 277: 130-186.
22. van Bokhoven JA, Lamberti C, *X-Ray Absorption and X-Ray Emission Spectroscopy: Theory and Applications*, John Wiley & Sons, Chichester, 2016.
23. Iwasawa Y, *XAFS Techniques for Catalysts, Nanomaterials, and Surfaces*, Springer, Berlin, 2016.
24. Ramaker D (2016) Novel XAS Techniques for Probing Fuel Cells and Batteries. In J. A. van Bokhoven and C. Lamberti (eds), X-Ray Absorption and X-Ray Emission Spectroscopy: Theory and Applications, John Wiley & Sons, Chichester, pp. 385-522.
25. Lamberti C, van Bokhoven JA (2016) X-Ray Absorption and Emission Spectroscopy for Catalysis. In J. A. van Bokhoven and C. Lamberti (eds), X-Ray Absorption and X-Ray Emission Spectroscopy: Theory and Applications, John Wiley & Sons, Chichester, pp. 353-383.

26. Kwak JH, Tonkyn RG, Kim DH et al (2010) Excellent activity and selectivity of Cu-SSZ-13 in the selective catalytic reduction of NO_x with NH_3. J. Catal., 275: 187-190.
27. Kwak JH, Tran D, Burton SD et al (2012) Effects of hydrothermal aging on NH_3-SCR reaction over Cu/zeolites. J. Catal., 287: 203-209.
28. Kwak JH, Lee JH, Burton SD et al (2013) A Common Intermediate for N_2 Formation in Enzymes and Zeolites: Side-On Cu–Nitrosyl Complexes. Angew. Chem. Int. Ed., 52: 9985-9989.
29. Paolucci C, Verma AA, Bates SA et al (2014) Isolation of the Copper Redox Steps in the Standard Selective Catalytic Reduction on Cu-SSZ-13. Angew. Chem.-Int. Edit., 53: 11828-11833.
30. Günter T, Carvalho HWP, Doronkin DE et al (2015) Structural snapshots of the SCR reaction mechanism on Cu-SSZ-13. Chem. Commun., 51: 9227-9230.
31. Janssens TVW, Falsig H, Lundegaard LF et al (2015) A Consistent Reaction Scheme for the Selective Catalytic Reduction of Nitrogen Oxides with Ammonia. ACS Catal., 5: 2832-2845.
32. Iwamoto M, Yahiro H, Tanda K et al (1991) Removal of nitrogen monoxide through a novel catalytic process .1. Decomposition on excessively copper-ion exchanged ZSM-5 zeolites. J. Phys. Chem., 95: 3727-3730.
33. Ahlquist M, Nielsen RJ, Periana RA et al (2009) Product Protection, the Key to Developing High Performance Methane Selective Oxidation Catalysts. J. Am. Chem. Soc., 131: 17110-17115.
34. Davies P, Snopwdon FF (1967) Production of oxygenated hydrocarbons. US Patent 3,326,956 1667.
35. Klier K (1982) Methanol synthesis. Adv. Catal., 31: 243-313.
36. Iwamoto M, Yahiro H, Torikai Y et al (1990) Novel preparation method of highly copper ion-exchanged ZSM-5 zeolites and their catalytic activities for NO decomposition. Chem. Lett., 1967-1970.
37. Iwamoto M, Yahiro H, Mizuno N et al (1992) Removal of nitrogen monoxide through a novel catalytic process .2. Infrared study on surface-reaction of nitrogen monoxide adsorbed on copper ion-exchanged ZSM-5 zeolites. J. Phys. Chem., 96: 9360-9366.
38. Li YJ, Hall WK (1990) Stoichiometric catalytic decomposition of nitric-oxide over Cu-ZSM-5 catalysts. J. Phys. Chem., 94: 6145-6148.
39. Li YJ, Hall WK (1991) Catalytic decomposition of nitric-oxide over Cu-Zeolites. J. Catal., 129: 202-215.
40. Shelef M (1995) Selective catalytic reduction of NO_x with N-free reductants. Chem. Rev., 95: 209-225.
41. Li JH, Chang HZ, Ma L et al (2011) Low-temperature selective catalytic reduction of NO_x with NH_3 over metal oxide and zeolite catalysts-A review. Catal. Today, 175: 147-156.
42. Kuroda Y, Kotani A, Maeda H et al (1992) The state of excessively ion-exchanged copper in mordenite - formation of tetragonal hydroxy-bridged copper-Ion. J. Chem. Soc. Faraday Trans., 88: 1583-1590.
43. Grünert W, Hayes NW, Joyner RW et al (1994) Structure, chemistry, and activity of Cu-ZSM-5 catalysts for the selective reduction of NO_x in the presence of oxygen. J. Phys. Chem., 98: 10832-10846.
44. Lamberti C, Bordiga S, Salvalaggio M et al (1997) XAFS, IR, and UV-vis study of the Cu^I environment in Cu^I-ZSM-5. J. Phys. Chem. B, 101: 344-360.
45. Lamberti C, Spoto G, Scarano D et al (1997) Cu^I-Y and Cu^{II}-Y zeolites: A XANES, EXAFS and visible-NIR study. Chem. Phys. Lett., 269: 500-508.
46. Lamberti C, Bordiga S, Zecchina A et al (1998) XANES, EXAFS and FTIR characterization of copper-exchanged mordenite. J. Chem. Soc. Faraday Trans., 94: 1519-1525.
47. Lamberti C, Palomino GT, Bordiga S et al (2000) Structure of homoleptic $Cu^I(CO)_3$ cations in Cu^I-exchanged ZSM-5 zeolite: An X-ray absorption study. Angew. Chem. Int. Edit., 39: 2138-2141.
48. Turnes Palomino G, Fisicaro P, Bordiga S et al (2000) Oxidation states of copper ions in ZSM-5 zeolites. A multitechnique investigation. J. Phys. Chem. B, 104: 4064-4073.
49. Turnes Palomino G, Bordiga S, Zecchina A et al (2000) XRD, XAS, and IR characterization of copper-exchanged Y zeolite. J. Phys. Chem. B, 104: 8641-8651.
50. Prestipino C, Berlier G, Llabrés i Xamena FX et al (2002) An in situ temperature dependent IR, EPR and high resolution XANES study on the NO/Cu^+-ZSM-5 interaction. Chem. Phys. Lett., 363: 389-396.
51. Giordanino F, Vennestrom PNR, Lundegaard LF et al (2013) Characterization of Cu-exchanged SSZ-13: a comparative FTIR, UV-Vis, and EPR study with Cu-ZSM-5 and Cu-β with similar Si/Al and Cu/Al ratios. Dalton Trans., 42: 12741-12761.
52. Fickel DW, Fedeyko JM, Lobo RF (2010) Copper Coordination in Cu-SSZ-13 and Cu-SSZ-16 Investigated by Variable-Temperature XRD. J. Phys. Chem. C, 114: 1633-1640.
53. Beale AM, Gao F, Lezcano-Gonzalez I et al (2015) Recent advances in automotive catalysis for NOx emission control by small-pore microporous materials. Chem. Soc. Rev., 44: 7371-7405.
54. van Bohkoven JA, Lamberti C (2016) X-ray absorption and emission spectroscopy for catalysis. In J.A. van Bokhoven and C. Lamberti (eds), X-Ray Absorption and X-ray Emission Spectroscopy: Theory and Applications, John Wiley & Sons, New York, pp. 354-383.
55. Singh J, Lamberti C, van Bokhoven JA (2010) Advanced X-ray absorption and emission spectroscopy: in situ catalytic studies. Chem. Soc. Rev., 39: 4754-4766.

56. McEwen JS, Anggara T, Schneider WF et al (2012) Integrated operando X-ray absorption and DFT characterization of Cu-SSZ-13 exchange sites during the selective catalytic reduction of NOx with NH_3. Catal. Today, 184: 129-144.
57. Bates SA, Verma AA, Paolucci C et al (2014) Identification of the active Cu site in standard selective catalytic reduction with ammonia on Cu-SSZ-13. J. Catal., 312: 87-97.
58. Doronkin DE, Casapu M, Gunter T et al (2014) Operando Spatially- and Time-Resolved XAS Study on Zeolite Catalysts for Selective Catalytic Reduction of NO_x by NH_3. J. Phys. Chem. C, 118: 10204-10212.
59. Giordanino F, Borfecchia E, Lomachenko KA et al (2014) Interaction of NH_3 with Cu-SSZ-13 Catalyst: A Complementary FTIR, XANES, and XES Study. J. Phys. Chem. Lett., 5: 1552-1559.
60. Borfecchia E, Lomachenko KA, Giordanino F et al (2015) Revisiting the nature of Cu-sites in activated Cu-SSZ-13 catalyst for SCR reaction. Chem. Sci., 6: 548-563.
61. Pluth JJ, Smith JV, Mortier WJ (1977) Positions of cations and molecules in zeolites with the chabazite framework. IV Hydrated and dehydrated Cu^{2+}-exchanged chabazite. Mat. Res. Bull., 12: 1001-1007.
62. Korhonen ST, Fickel DW, Lobo RF et al (2011) Isolated Cu^{2+} ions: active sites for selective catalytic reduction of NO. Chem. Commun., 47: 800-802.
63. Pierloot K, Delabie A, Groothaert MH et al (2001) A reinterpretation of the EPR spectra of Cu(II) in zeolites A, Y and ZK4, based on ab initio cluster model calculations. Phys. Chem. Chem. Phys., 3: 2174-2183.
64. Deka U, Juhin A, Eilertsen EA et al (2012) Confirmation of Isolated Cu^{2+} Ions in SSZ-13 Zeolite as Active Sites in NH_3-Selective Catalytic Reduction. J. Phys. Chem. C, 116: 4809-4818.
65. Kwak JH, Varga T, Peden CHF et al (2014) Following the movement of Cu ions in a SSZ-13 zeolite during dehydration, reduction and adsorption: A combined in situ TP-XRD, XANES/DRIFTS study. J. Catal., 314: 83-93.
66. Llabrés i Xamena FX, Fisicaro P, Berlier G et al (2003) Thermal reduction of Cu^{2+}-mordenite and Re-oxidation upon interaction with H_2O, O_2, and NO. J. Phys. Chem. B, 107: 7036-7044.
67. Kispersky VF, Kropf AJ, Ribeiro FH et al (2012) Low absorption vitreous carbon reactors for operando XAS: a case study on Cu/Zeolites for selective catalytic reduction of NOx by NH_3. Phys. Chem. Chem. Phys., 14: 2229-2238.
68. Alayon EMC, Nachtegaal M, Ranocchiari M et al (2012) Catalytic Conversion of Methane to Methanol Using Cu-Zeolites. Chimia, 66: 668-674.
69. Alayon EMC, Nachtegaal M, Bodi A et al (2014) Reaction Conditions of Methane-to-Methanol Conversion Affect the Structure of Active Copper Sites. ACS Catal., 4: 16-22.
70. Wulfers MJ, Teketel S, Ipek B et al (2015) Conversion of methane to methanol on copper-containing small-pore zeolites and zeotypes. Chem. Commun., 51: 4447-4450.
71. Periana RA, Taube DJ, Gamble S et al (1998) Platinum catalysts for the high-yield oxidation of methane to a methanol derivative. Science, 280: 560-564.
72. Rosenzweig AC, Frederick CA, Lippard SJ et al (1993) Crystal-structure of a bacterial nonheme iron hydroxylase that catalyzes the biological oxidation of methane Nature, 366: 537-543.
73. Sazinsky MH, Lippard SJ (2015) Methane Monooxygenase: Functionalizing Methane at Iron and Copper. In P. M. H. Kroneck and M. A. Sosa Torres (eds), Sustaining Life on Planet Earth: Metalloenzymes Mastering Dioxygen and Other Chewy Gases. Metal Ions in Life Sciences, Springer, Berlin, pp. 205-256.
74. Woertink JS, Smeets PJ, Groothaert MH et al (2009) A $[Cu_2O]^{2+}$ core in Cu-ZSM-5, the active site in the oxidation of methane to methanol. Proc. Natl. Acad. Sci. U. S. A., 106: 18908-18913.
75. Groothaert MH, van Bokhoven JA, Battiston AA et al (2003) Bis(μ-oxo)dicopper in Cu-ZSM-5 and its role in the decomposition of NO: A combined in situ XAFS, UV-Vis-Near-IR, and kinetic study. J. Am. Chem. Soc., 125: 7629-7640.
76. Yamaguchi A, Shido T, Inada Y et al (2000) Time-resolved DXAFS study on the reduction processes of Cu cations in ZSM-5. Catal. Lett., 68: 139-145.
77. Yamaguchi A, Inada Y, Shido T et al (2001) Time-resolved energy-dispersive XAFS study on the reduction process of Cu-ZSM-5 catalysts. J. Synchrot. Radiat., 8: 654-656.
78. Yamaguchi A, Shido T, Inada Y et al (2001) In situ time-resolved energy-dispersive XAFS study on the reduction processes of Cu-ZSM-5 catalysts. Bull. Chem. Soc. Jpn., 74: 801-808.
79. Alayon EMC, Nachtegaal M, Bodi A et al (2015) Bis(μ-oxo) versus mono(μ-oxo)dicopper cores in a zeolite for converting methane to methanol: an in situ XAS and DFT investigation. Phys. Chem. Chem. Phys., 17: 7681-7693.
80. Grundner S, Markovits MAC, Li G et al (2015) Single-site trinuclear copper oxygen clusters in mordenite for selective conversion of methane to methanol. Nat. Commun., 6: 9.
81. Horn R, Schlogl R (2015) Methane Activation by Heterogeneous Catalysis. Catal. Lett., 145: 23-39.